VALIDATION OF RADIATED SOUND FROM A MACH 0.75 JET

Odenir de Almeida
EMBRAER – Empresa Brasileira de Aeronáutica S.A., São José dos Campos – SP – Brazil.
odenir.almeida@embraer.com.br

Carlos Roberto Ilário da Silva
EMBRAER – Empresa Brasileira de Aeronáutica S.A., São José dos Campos – SP – Brazil.
carlos.ilario@embraer.com.br

Abstract. In this paper, the validation of the noise generated by a single-stream jet operated at subsonic Mach 0.75 has been performed using Computational Fluid Dynamics (CFD) in conjunction with Computational Aeroacoustics (CAA) and semi-empirical methods. First of all, 2D axisymmetric and 3D simulations were applied to characterize the flow dynamics of the jet. Experimental data available were used to corroborate the numerical results. Once the flow field was well simulated the identification of jet´s noise sources could be evaluated by two distint methodologies both available in CAA++ software: a) an analytical propagation solver via Curle's solution; b) a non-linear acoustic solver (NLAS) and Ffowcs Williams-Hawkings. Empirical methods for jet noise prediction have been applied to complement the analysis and to validate the sound pressure level (SPL) spectra. Such numerical results have been compared to experimental acoustic data.

Keywords: noise sources, jet flow, fluid dynamics, aeroacoustics.

1. Introduction

During the last decade's aircraft noise has been reduced by almost 20 decibels with the implementation of new technologies for engine and airframe. Nevertheless, engine noise is still the most dominant source from today's aircraft. Despite significant progress in reducing engine noise, further improvements are necessary as aircraft noise requirements are becoming more stringent.

Engine noise sources can be attributed mainly to turbomachinery noise (especially fan noise), combustor noise and jet noise. The technologies applied to fan and jet components are the most significant and have been the focus of most of the engine noise research in recent years. Many of these researches aimed at understanding the mechanisms of noise generation and propagation.

Specifically for jet noise, recent developments deal not only with scale model tests (experimental) but also with numerical models with different degrees of sophistication. These numerical models can be since very simple empirical codes, based on experimental database, until advanced computational aeroacoustics (CAA) codes, based on a complete description of the fluid dynamics through sets of partial differential equations. Nevertheless, when exclusively talking about CAA, it's quite true that these methods must evolve significantly in order to have a good and reliable applicability in industrial flows.

On the other hand, with the development in computational methodologies and the need of industrial tools to predict noise, these aeroacoustics codes have been applied consecutively to the noise prediction of free shear flows like jets and pure mixing layers. Indeed, in the literature is possible to find many variants of aeroacoustics methodologies being applied for jet noise prediction.

It's important to emphasize here the two approaches largely used for noise prediction, which are: 1) noise source characterization via CFD modeling; 2) noise propagation. The first approach is discussed just in the sequence.

Taking into account the physics employed in these models it's possible to classify and consider those ones with potential for industrial applications, based on requirements such as capability of predicting broadband and tonal contents, accuracy on predicting noise levels and time and power computer efficiency.

Figure (1) shows schematically the physics representation for the most known CFD methodologies available for jet noise prediction (source characterization). Putting these methods in a scale, the direct numerical simulation (DNS) is the state of art and is longer the most physics representative for noise prediction, since all scales of the turbulent flow field are computed. However, it's not feasible when dealing with industrial flows at high Mach numbers due to limitations on computational resources to accomplish such task. In sequence, large eddy simulation (LES) is less restringing than DNS, but less physics is incorporated for modeling, since the smallest scales are computed by a sub-grid model. For jet noise prediction, LES is still not doable depending on the Mach number. Most recent works point out to different applications of hybrid methods in aeroacoustics, but these methods are still expensive and very sensitive to numerical parameters. Reynolds Averaged Navier-Stokes (RANS) method, on the other hand, is much known and computationally cheap to perform. Obviously, this methodology doesn't provide unsteady fluctuations of variables in the flow field. However, methods as MGB – Mani (1976), Balsa (1977) and Gliebe (1978) in 80's were based on RANS simulations to evaluate noise sources.

Despite these methodologies are consecrated, for industrial application, they could not be applied as a stand-alone method for noise prediction, unless the observer is very close to the source. Indeed, basically due to the need of predicting noise levels at high distance from the noise source, industrial applications put more challenges for numerical modeling. At this point, the second approach (previously announced) should take place as an alternative method for long distance propagation of acoustics waves, which are obviously generated by the methodologies presented for noise source characterization.
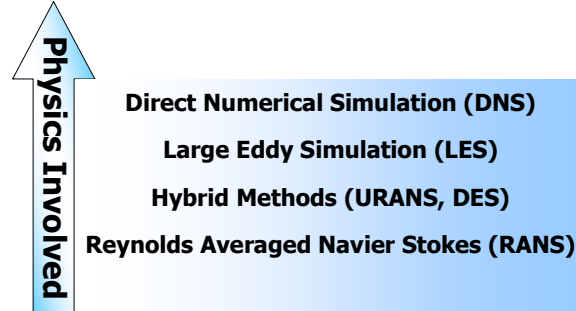
Figure 1. Physics representation for jet noise prediction.

The original idea comes back with the coupling between the methodologies exposed previously with analytical propagation models, as Lighthill's (Lighthill (1952)) or Curle's equations (Curle (1970)) (volumetric source integration) or even Ffowcs-Williams/Hawking equation (surface source integration) – Ffowcs & Hawking (1969).

More recently, another class of computational aeroacoustics method was presented by Batten et al. (2004), based on non-linear disturbance equations. This methodology is used to combine advantageous features from both conventional acoustic analogy frameworks and hybrid Reynolds-averaged Navier-Stokes (RANS)/Large Eddy Simulation (LES) methods. It turns to an alternative framework for partially resolving, and partially modeling, flow-generated acoustics.

This paper deals with the aeroacoustics validation of radiated sound from a Mach 0.75 jet. Numerical simulations have been carried out using the commercial software CFD++ in conjunction with CAA++, which employs two distinct methods for noise prediction: a) an analytical propagation solver via Curle's equation solution; b) a non-linear acoustic solver (NLAS) and Ffowcs-Williams/Hawking equation. Empirical methods (ESDU database) for jet noise prediction have been applied to complement the analysis and to validate the sound pressure level (SPL) spectra. Such numerical results have been compared to experimental acoustic data.

2. Problem Description & Computational Details

In order to validate the aeroacoustics code employed in this work, a single stream jet operating at subsonic speed of Mach 0.75 was investigated. Some experimental data for the jet's fluid dynamics is available in the literature from the work of Andersson et al (2005). Acoustic data for this configuration is also available but not completely recoverable from public literature. To overcome this leak of data for comparison, the ESDU data program package number 01004 has been applied to predict the 1/3 Octave Band Sound Pressure Level (SPL) at different emission angles measured from the jet centerline.

Table 1 presents the inlet conditions for the jet according to Andersson et al (2005).

Table 1. Inlet conditions for the Mach 0.75 subsonic jet.

Ambient Conditions: P_∞ = 101.3 kPa and T_∞ = 288 K
D_j = 50.0 mm   (jet's diameter)

T_j (K)	U_j (m/s)	Total Pressure (kPa)	Total Temperature (K)
288	255	147.16	320.4

Figure 2(a) and (b) shows the geometric dimensions of the computational domain and the mesh resolution used for the (2D) two-dimensional axis-symmetric RANS simulations.

The computational mesh used for 2D calculation consists of 88424 quadrilaterals elements clustered close to the nozzle wall and concentrated to the shear layer of the jet. A minimum stretch was used to expand the mesh in the axial and radial directions.

Figure 3(a), (b) and (c) shows the mesh resolution for the complete (3D) three-dimensional domain, a slice of the calculation domain in the nozzle region at x = 0 and the mesh resolution used to discretize the nozzle geometry. This 3D RANS mesh was generated using 1.530.072 hexahedral cells, clustered to the nozzle wall and refined in the full wake of the jet.
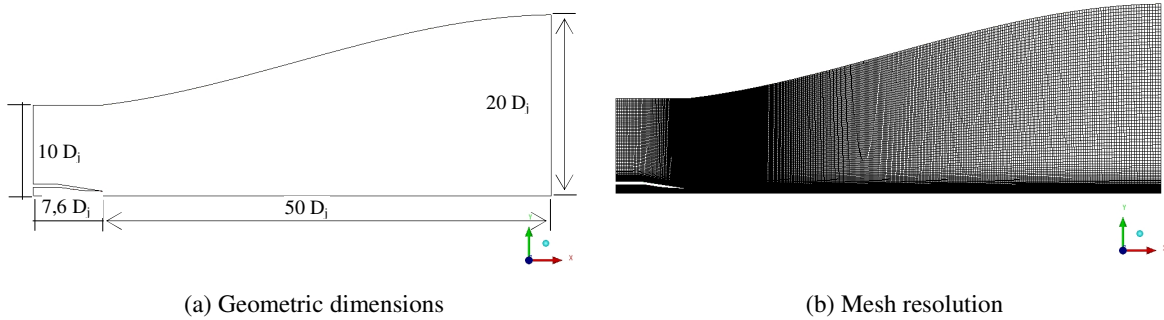
(a) Geometric dimensions   (b) Mesh resolution
Figure 2. 2D Computational domain.
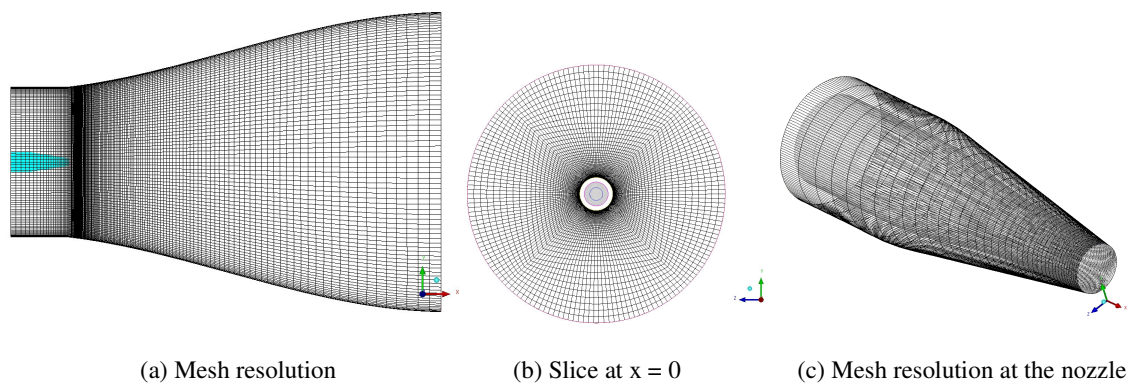
(a) Mesh resolution   (b) Slice at x = 0   (c) Mesh resolution at the nozzle
Figure 3. 3D computational domain – Mesh details.

3. Numerical Method for Fluid Dynamics

In the present work, in order to run the 2D and 3D RANS simulations a non-linear $k-\varepsilon$ closure was employed, named $k-\varepsilon$ cubic model. The formulation to obtain Reynolds-stress tensor is defined via a tensorial expansion, cubic in the mean strain and vorticity tensors.

The stresses are related to the mean strain and vorticity using the quadratic model of Shih et al. (1993) with the cubic extension proposed by Lien and Leschziner (1996). More details about the model are given in Goldberg et al. 2000.

4. Numerical Method for Aeroacoustics

Once the flow field was well characterized the identification of jet's noise sources could be evaluated by two distint methodologies both available in CAA++ software: a) an analytical propagation solver via Curle's solution; b) a non-linear acoustic solver (NLAS) and Ffowcs Williams-Hawkings (FWH) propagation model.

For the first approach, the 2D axis-symmetric RANS mean field, Reynolds-stress and dissipation rate data are interpolated (expanded) onto an acoustics 3D mesh (Figure 4) and farfield data at the outer boundaries are then set from the interpolated RANS mean field data at those locations. Then, the empirical wave propagation solver is used to evaluate the volumetric noise sources and to propagate acoustics perturbations to the farfield – section 4.1.

In the second approach, two possibilities are available for taking into account the RANS solution. It's possible to get the 2D axis-symmetric RANS results (mean field, Reynolds-stress and dissipation rate) and interpolate onto a 3D acoustics mesh for NLAS. On the other hand, it's also possible to get a 3D RANS result and interpolate onto a 3D acoustics mesh. Both procedures were employed in this work in order to verify which one is best suitable for jet noise prediction. Details about NLAS solver and the acoustics mesh are found in section 4.2.

4.1 Analytical Wave Propagation Solver

The analytical wave propagation solver provides an approximate but rapid means of evaluate far-field noise from conventional RANS solutions. This solver can be considered an analytical model which works by reconstructing the sound-generating velocity fluctuations from the statistics contained within the given turbulence solution. Since these

statistics describe the full spectrum of turbulence, there is no limit to the frequencies that can be extracted using an analytic wave propagation model. The proposed model can therefore be used as a stand-alone tool to provide full-spectrum predictions, or in conjunction with a separate numerical solver, to provide a description of the unresolved frequencies. The model is based on a form of Lighthill's equation, according to Equations (1) and (2).

$$\frac{\partial^2 \rho'}{\partial t^2} - c_0^2 \frac{\partial^2 \rho'}{\partial x_i^2} = \frac{\partial^2 T_{ij}}{\partial x_i \partial x_j} \tag{1}$$

where:

$$T_{ij} = \rho u_i u_j - \tau_{ij} + (p - c_\infty^2 \rho)\delta_{ij} \tag{2}$$

The right-hand side terms are assumed to be known and independent of the left-hand side, which then simply represents a wave-propagation operator. A solution to this equation was proposed in 1970 by Curle (1970):

$$\rho(x_j,t)' = \frac{1}{4\pi c_\infty^2} \iiint \frac{1}{r} \frac{\partial^2 T_{ij}}{\partial y_i \partial y_j} dV - \frac{1}{4\pi} \iint \left(\frac{1}{r} \frac{\partial \rho}{\partial n} + \frac{1}{r^2} \frac{\partial r}{\partial n} \rho + \frac{1}{c_\infty r} \frac{\partial r}{\partial n} \frac{\partial \rho}{\partial \tau} \right) dS \tag{3}$$

where n defines the local surface normal. A solution to Curle's equation, which is valid for arbitrary r can be written as (see, for example, Larsson (2002)):

$$p'(x_i,t) = \frac{1}{4\pi} \iiint \left[\frac{l_i l_j}{c_\infty^2 r} \frac{\partial^2 T_{ij}}{\partial t^2} + \frac{3l_i l_j - \delta_{ij}}{c_\infty r^2} \frac{\partial T_{ij}}{\partial t} + \frac{3l_i l_j - \delta_{ij}}{r^3} T_{ij} \right] dV +$$
$$\frac{1}{4\pi} \iint l_i n_j \left[\frac{1}{c_\infty r} \left(\frac{\partial p}{\partial t} \delta_{ij} - \frac{\partial \tau_{ij}}{\partial t} \right) + \frac{p\delta_{ij} - \tau_{ij}}{r^2} \right] dS \tag{4}$$

Given a suitable mathematical model for the terms on the right-hand side, the previous equation can be used to determine the resulting acoustic pressures as a function of position (x_i) and time (*t*). These sources are determined in the model using an assumption that the pressure fluctuations on the right-hand side, corresponding to monopole sources (such as mass sources/sinks) and dipole sources (such as oscillating surfaces) are zero. The quadrupole terms, corresponding to the fine-scale turbulent fluctuations are determined by a mathematical model that reconstructs the fluctuating velocity field from a given set of turbulence statistics (the details of this reconstruction are given in the section below). It's worth noting that an important limitation of this model is that it ignores the presence of walls, implying that waves are not blocked, reflected from, or refracted around solid obstacles. The proposed model is therefore best suited for problems involving free shears or jets.

In order to run this model a 3D mesh is required since Equation (4) is integrated over discrete volumes. As stated above, the presence of walls was ignored, i.e. the simulations were run without the nozzle. To accomplish this task, a separate acoustics mesh was generated through a cutting process from the original 3D RANS mesh.

Figure 4 shows the acoustics volumetric mesh for the empirical wave propagation solver with 1.528.967 hexahedral cells (50D_j in x-direction and 10D_j in the y-direction).
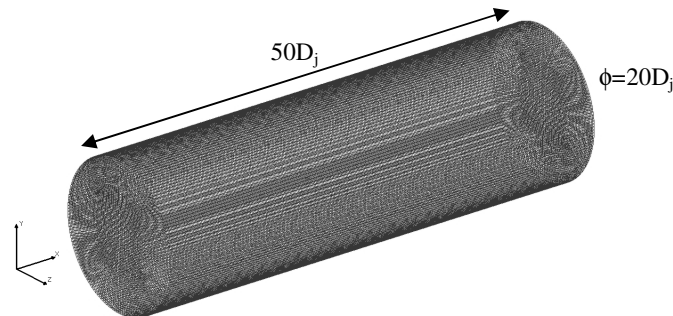
Figure 4. Acoustics mesh for the empirical wave propagation solver.

4.2 Non Linear Acoustic Solver (NLAS)

The rationale for the non-linear acoustics solver proposed in Batten et al. (2002) is that the fine scale turbulent motions giving rise to the acoustic sources must (at some level) be modeled, however, flows involving coherent structures or resonance require predictions of noise radiated from the interaction of these large-scale structures.

The Non-Linear Acoustics Solver (NLAS) is a numerical acoustics solver designed to model noise generation and transmission from an initial statistically-steady model of a turbulent flow - data that can be provided by a simple RANS model. This initial step provides a baseline description of the mean flow as well as a statistical description of the superimposed turbulent fluctuations. The NLAS then uses a reconstruction procedure to generate noise sources from the given set of statistics and allows the resulting propagation of the pressure disturbances to be simulated using a high-resolution solver. The NLAS routine can be used to propagate the resolved-scale pressure disturbances on the original (RANS) mesh or, following interpolation of the acoustics output data, on a separate acoustics mesh.

NLAS is a low-diffusion solver which accounts for noise-generation from structures at sub-grid scales. It relies on the concept of disturbances or perturbations computed around a pre-determined mean flow, using statistical models for the sub-grid noise sources, obtained from the same a priori mean-flow computation. The NLAS solver considers a perturbation to the Navier-Stokes equations, in which quantities are split into mean and fluctuating parts: $\phi = \overline{\phi} + \phi'$. Substituting into the Navier-Stokes equations and rearranging for fluctuation and mean quantities gives a system of perturbation equations referred to as non-linear disturbance equations (NLDE):

$$\underbrace{\frac{\partial q'}{\partial t} + \frac{\partial F_i'}{\partial x_i} - \frac{\partial (F_i^v)'}{\partial x_i}}_{} = \underbrace{-\frac{\partial \overline{q}}{\partial t} - \frac{\partial \overline{F_i}}{\partial x_i} + \frac{\partial \overline{F_i^v}}{\partial x_i}}_{} \tag{5}$$

where:

$$q = \begin{bmatrix} \rho' \\ \overline{\rho}u_j' + \rho'\overline{u}_j + \rho'u_j' \\ e' \end{bmatrix}, \qquad (F^v)_i' = \begin{bmatrix} 0 \\ \tau_{ij}' \\ -\theta_i' + u_k'\overline{\tau}_{ki} + \overline{u}_k\tau_{ki}' \end{bmatrix}, \tag{6}$$

$$F_i' = \begin{bmatrix} \overline{\rho}u_i' + \rho'\overline{u}_i \\ \rho'\overline{u}_i\overline{u}_j + \overline{\rho}\overline{u}_iu_j' + \overline{\rho}u_i'\overline{u}_j + p'\delta_{ij} \\ u_i'(\overline{e} + \overline{p}) + \overline{u}_i(e' + p') \end{bmatrix} + \begin{bmatrix} \rho'u_i' \\ \overline{\rho}u_i'u_j' + \rho'u_i'\overline{u}_j + \rho'\overline{u}_iu_j' + \rho'u_i'u_j' \\ u_i'(e' + p') \end{bmatrix} \tag{7}$$

Neglecting density fluctuations and taking time averages gives:

$$\Rightarrow \quad \overline{LHS} = \overline{RHS} = \frac{\partial R_i}{\partial x_i}, \quad R_i = \begin{bmatrix} 0 \\ \overline{\rho u_i' u_j'} \\ c_p \overline{\rho T' u_i'} + \overline{\rho u_i' u_k' \overline{u}_k} + \frac{1}{2} \overline{\rho u_i' u_k' u_i'} + \overline{u_k' \tau_{ki}} \end{bmatrix} \tag{8}$$

The above terms correspond to the standard Reynolds-stress tensor and turbulent heat fluxes. The key step in NLAS is to obtain these unknown terms in advance from a classical RANS method. Subsequently, a synthetic reconstruction of the unresolvable (short wavelength) contribution to these terms can then be generated and used to form the sub-grid source terms for the NLAS simulation. With both mean levels and sub-grid sources established, time-dependent computations can then be made to determine the transmitted perturbations about this mean using the above set of disturbance equations.

The use of an initial RANS calculation to provide mean-flow and statistical data, allows the reduction of meshing requirement for the expensive (time dependent) part of the acoustics simulation process. NLAS is able to operate on a reduced sub-domain, with absorbing far-field boundaries defined by a truncated subset of the original RANS calculation, which provides not only turbulence statistics, but also spatially varying mean-field data that can be used to place the outer boundary conditions much closer to the regions of interest than would be possible with a single, transient time-domain computation.

Figure 5 shows the acoustics volumetric mesh for the non-linear acoustics solver with 2.857.904 hexahedral cells, due to uniform spacing in the jet's wake. The time marching for NLAS was of order 1×10^{-5} (s) reaching 0.5 (s) of global time simulation (50000 time steps performed). This mesh domain has the same dimension of Figure 2(a).
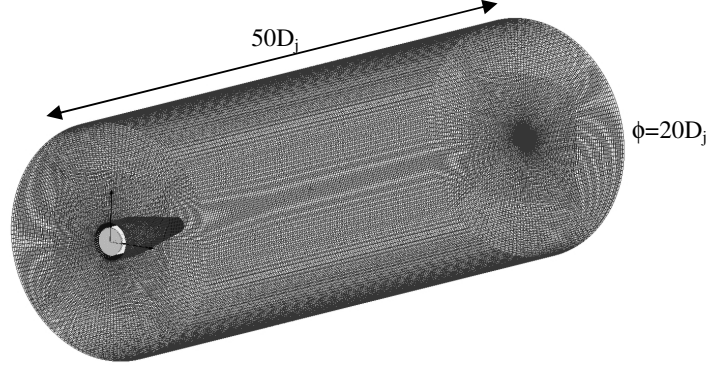
Figure 5. Acoustics mesh for the non-linear acoustic solver (NLAS).

4.3 Synthesis of Turbulence

In NLAS, the larger-scale fluctuations are represented directly, hence a synthetic reconstruction of the unresolvable scales is necessary. The model employed is based on the idea of Smirnov et al. (2001) embedding a tensor scaling based on a similarity transformation of the Reynolds-stress tensor that is able to account for turbulence anisotropy. The model used in CAA++ is a variant of this model, according to Batten et al. (2002, 2004).

$$u_i(x_j,t) = a_{ik}\sqrt{\frac{2}{N}}\sum_{n=1}^{N}\left[p_k^n\cos(\hat{d}_j^n\hat{x}_j + \omega^n\hat{t}) + q_k^n\sin(\hat{d}_j^n\hat{x}_j + \omega^n\hat{t})\right] \tag{9}$$

where:

$$c^n = \sqrt{3\overline{u_l'u_m'}d_l^n d_m^n / 2d_k^n d_k^n}, \quad p_i^n = \varepsilon_{ijk}\zeta_j^n d_m^n, \quad q_i^n = \varepsilon_{ijk}\xi_j^n d_m^n \tag{10}$$

$$\hat{x}_j = 2\pi x_j / L, \quad \hat{t} = 2\pi t / \tau, \quad \hat{d}_j^n = d_j^n \frac{V}{c^n}, \quad V = L / \tau \tag{11}$$

$$\zeta_i^n, \xi_i^n = N(0,1), \quad \omega^n = N(1,1), \quad d_i^n = N(0,1/2) \tag{12}$$

In the above expressions, N (α,β), implies a Gaussian normal variable with a mean of α, and standard deviation β. The same approach is valid for ξ, ω and d, as stated in (12). The time and space correlations are modeled by scaling time and distance coordinates by the local turbulence time scale, τ, and velocity scale, c^n. The c^n scaling preferentially increases the correlation distances in directions aligned with larger root-mean-square (rms) velocity fluctuations, whilst diminishing correlation distances in directions with smaller rms fluctuations. The final set of time-dependent velocity fluctuations are then determined using a tensor scaling based on the Cholesky decomposition (a_{ik}) of the local Reynolds-stress tensor.

For completeness of this model, please refer to references Batten et al. (2002, 2004) and Smirnov et al. (2001).

4.4 Ffowcs Williams-Hawkings (FWH) propagation model

The acoustics post-processing of the computed unsteady flow field (evaluated by NLAS) is performed by integration of Ffowcs-Williams/Hawking equation – FfowcsWilliams & Hawking (1969). Such approach provides the pressure radiated by a volume of perturbed fluid, starting from the computed perturbations on a closed control surface surrounding this volume.

Figure 5 illustrates an example of Ffowcs-Williams/Hawking control surface used in the calculations. In summary, this method uses time-dependent surface data to solve the Ffowcs-Williams/Hawking equation for arbitrary observer points. The observer points are not required to lie within the computational mesh. However, a control surface mesh is needed to store pressure fluctuations.

The time step used to store data and to solve FWH equations was kept constant and equal to 1×10^{-5} (s). The mesh used has a streamwise resolution of about 0.01 m near the jet exit (the most important region in this flow). A sound wave (assuming c_0 is 340m/s and neglecting mean convection) will travel across one cell in approximately 2e-5s. This local Courant condition of unity (in the region of interest) is a good condition to aim for, as it provides an accurate means of convecting the acoustic waves.
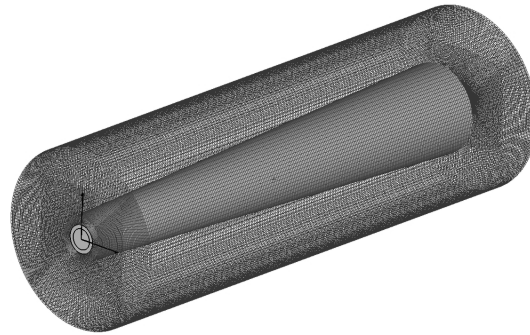
Figure 6. Acoustics surface control for integration of Ffowcs-Williams/Hawking equation.

5. Numerical Results

This section shows the numerical results obtained in this work. 2D axisymmetric and 3D simulations were applied to characterize the flow dynamics of the jet. Experimental data available from Andersson et al (2005) were used to corroborate the numerical results. With the flow field well simulated the identification of jet's noise sources could be evaluated by the methodologies previously presented.

5.1 Jet Fluid Dynamics

Results from the Reynolds-average Navier-Stokes (RANS) simulations for the Mach 0.75 jet were validated through the analysis of the centerline velocity distribution. This parameter is essential to demonstrate how the jet expands to a uniform medium (spreading rate), giving information about the potential core length and behavior of the mixing layer. Indeed, these parameters basically determine the characteristics of the noise sources and play important hole in the noise emission angles (directivity) of the jet. Thus, the better a RANS simulation is obtained at this step, the better will be the noise prediction when applying the methodologies exposed herein.

Figure 7 shows the centerline velocity distribution for both 2D axis symmetric and 3D RANS simulations. Despite the results are showed only for the extension of 12 jet diameters in the wake, it's possible to see that the core length is not quite well predicted by RANS modeling. However, the rate of velocity decay tends to be better predicted. This discrepancy in the prediction of the potential core length translates in a shift about the location of maximum turbulence intensity and has influence in the noise prediction.
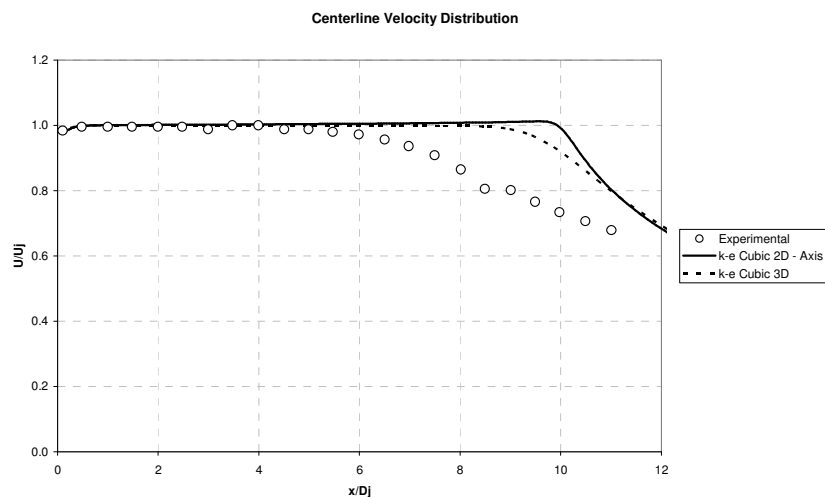
Figure 7. Centerline velocity distribution.

Since 3D RANS simulations provided better fluid dynamics results, the acoustics results obtained from 2D simulations will not be presented herein for brevity purposes. Results for acoustics will be presented considering only 3D RANS simulations as the startup process.

5.2 Jet Acoustics

As stated before, in order to produce an accurate acoustics simulation, which includes the correct attenuation of radiated sound waves, the acoustics data obtained from 3D RANS simulation was interpolated onto a full three-dimensional acoustic mesh – Figure 5.

The next section presents the farfield sound pressure levels evaluated by the two methodologies available in CAA++.

5.2.1 Farfield Sound Pressure Levels

Numerical predicted farfield sound pressure levels (SPL) are presented in Figure 8. The experimental spectra (SPL) are not available for the investigated emission angles (60º, 80º, 100º and 120º) measured from the jet exhaust. In order to validate the numerical data, the ESDU empirical code A98019 was used to compute SPL at given locations. These results are assumed to be trustful due to the inherent accuracy of the prediction method (± 3 dB). This approach was considered acceptable by the authors since the results should not be out of 3 dB from the original experimental data, if they exist.

The sound pressure levels were calculated for farfield observer locations placed in an arc of $30D_j$ from the nozzle exit plane at 4 distinct emission angles (60º, 80º, 100º and 120º).

(a) 60º

(b) 80º

(c) 100º

(d) 120º
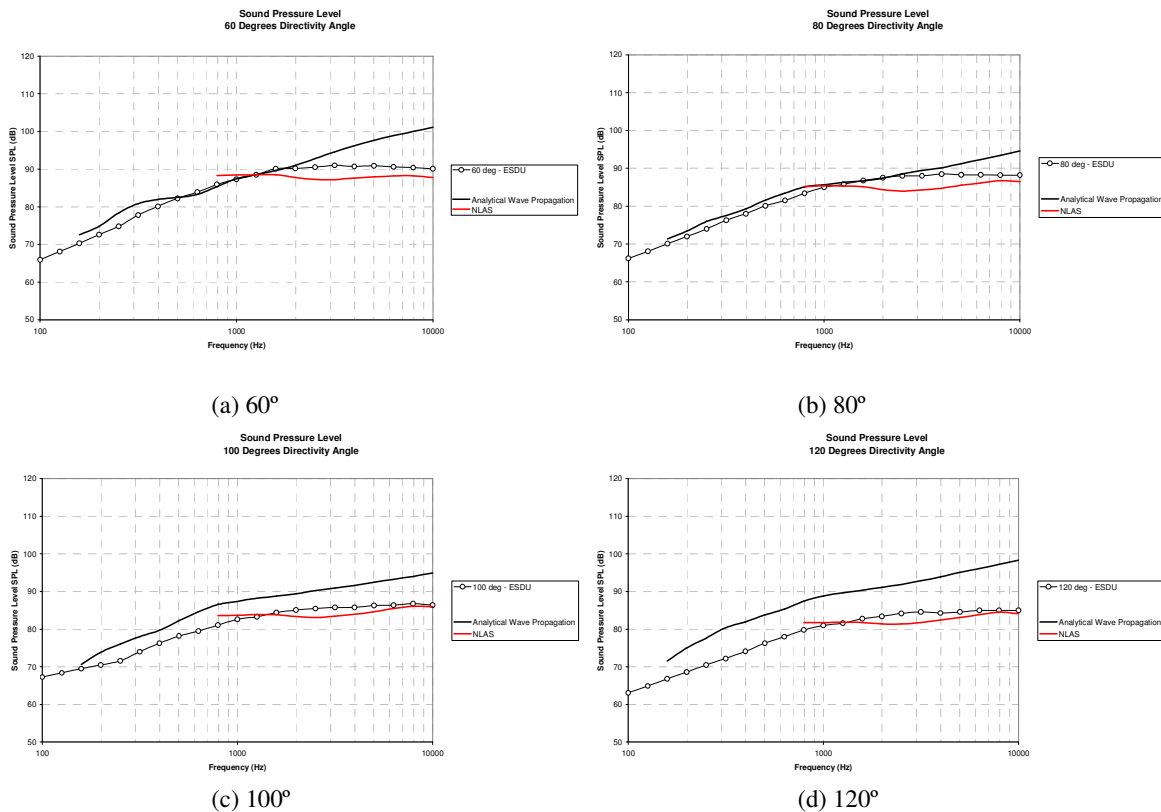
Figure 8. Farfield sound pressure levels in microphone location $30D_j$ from the nozzle exit plane – different emission angles (60º, 80º, 100º and 120º).

The variation of spectra with emission angles to the jet axis are not well predicted, particularly for the mid to the high frequencies (above 1000 Hz). Especially for frequencies above 2000 Hz the analytical wave propagation solver did provide a considerable increase in the spectrum slope. On the other hand the non-linear acoustic solver (NLAS) was more prone to capture frequencies above 1000 Hz within an acceptable dispersion range. However, it's important to emphasize that the NLAS was not able to capture with good resolution low frequencies (below 1000 Hz). This should

be attributed to the time domain sample, which is not large enough to provide good spectral resolution at low frequencies.

Another important aspect noted in the spectra is the increase in the absolute noise levels for the emission angles for frequencies above 2000 Hz, predicted with the analytical wave propagation solver. This systematic trend has been observed during applications of the solver for this class of problem and is explained as follows.

It's important to emphasize that the analytical wave propagation solver has no limit on the frequency range it can reproduce, however, a common consideration is the size of time-step employed. Often, signals in excess of a few thousand Hertz are not of interest and so the discrete sampling rate used (the choice of time-step) places a practical limit on the data ultimately computed from signal processing the output of such a tool.

For situations in which the time-step is sufficiently small to resolve most or all of the modeled energy contained in the turbulence statistics, no filtering is needed. However, if a significant amount of modeled energy remains in higher frequencies, this can be removed by source-term filtering.

To avoid such aliasing errors, it is necessary to remove, from the acoustic source terms, that energy which gives rise to signals that cannot be resolved at the user-selected sampling rate or time step. It should be noted that this filtering operation removes energy from the system, so that overall sound-pressure levels will be under-estimated. However, this is an appropriate choice if one needs to visualize acoustic energy over a restricted portion of the energy-containing frequency range.

At the time of these simulations, the filtering process was not available in the analytical propagation solver. Based on the discussion above, it's sure that the results presented in figure 8 are contaminated with energy at high frequencies that could not be modeled. Applications of this filtering process in other subsonic jet cases show considerable improvements in the SPL prediction all over the spectrum up to 10 Khz.

Finally, for the non-linear acoustic solver (NLAS), it is important to keep in mind that the mesh resolution and the time step both play an important role in the noise prediction. With the meshes used for the cases investigated the frequency range of interest lies between 100 Hz and 1000 Hz. For higher frequencies, a finer mesh and a smaller time discretization would be beneficial, however, work is also in progress to address the issue of noise source filtering with numerical propagation solvers.

6. Conclusions

This paper has considered some practical applications of aero-acoustics tools in the validation of the noise generated by a single-stream jet operated at subsonic Mach 0.75. Two distinct methodologies have been applied, based on analytical wave propagation via solution of Curle's equation and through the use of a non-linear acoustic solver via solution of viscous disturbance equations and turbulence synthesis of small scales present in the flow.

In this work, the sound pressure levels (SPL), obtained with the analytical wave propagation solver, showed a reasonable agreement when compared with ESDU data spectra, for a frequency range of 100 Hz up to 1000 Hz, showing potential for application in industrial jet-flows noise prediction. Some problems regarding sampling rate has been pointed out as crucial for jet noise prediction. Improvements in the model have been tested (not in this work) using a filter process to remove energy from the system.

Also, a non-linear acoustic solver (NLAS) has been used for comparison purposes. The numerical results obtained with NLAS are strongly influenced by numerical parameters such as mesh spacing and time resolution. However, reasonable agreement was found for frequencies above 1000 Hz. Future work will address the issue of improving the noise source models in such numerical solvers.

In summary, for the cases investigated it could be stated that the tools employed gave reasonable results for certain frequencies range in the validation of the noise generated by subsonic jet. The aerocoustics results obtained in this work are within a range of ± 10 dB.

7. Acknowledgments

8. References

Tam, C. K., "Advances in Numerical Boundary Conditions for Computational Aeroacoustics", American Institute of Aeronautics and Astronautics, AIAA paper-1774, pp. 1-16.

Tam, C. K., "Computational aeroacoustics: An overview of computational challenges and applications", International Journal of Computational Fluid Dynamics, Vol 18 (6), Aug 2004, pp. 547-567.

Tam, C. K., "Computational aeroacoustics: Issues and Methods", AIAA Journal, Vol 33 (10), October 2005, pp. 1788-1796.

Goldberg, U., Batten, P., Palaniswamy, S., Chakravarthy, S., and Peroomiam, O., "Hypersonic Flow Predictions Using Linear and Nonlinear Turbulence Closures", Journal of Aircraft, Vol 37, No. 4, 2000, pp. 671-675.

Shih, T. H., Lumley, J. L., Zhu, J., "A Realizable Reynolds Stress Albebraic Equation Mode", NASA TM-105993, 1993.

Lien, F. S., Leschziner, M. A., "Low-Reynolds number eddy-viscosity modelling based on non-linear stress-strain/vorticity relations". In: Rodi, W. and Bergeles, G. (eds), Engineering Turbulence Modelling and Experiments 3, Elsevier, Amsterdam, 1996, pp. 91-100.

Batten, P., Ribaldone, E., Casella, M., Chakravarthy, S., "Towards a Generalized Non-Linear Acoustics Solver," *10th AIAA/CEAS Aeroacoustics Conference*, AIAA 2004-3001, City, DC, 2004.

Batten, P., Goldberg, U., Chakravarthy, S., Reconstructed Sub-Grid Methods for Acoustics Predictions at all Reynolds Numbers, AIAA-2002-2511, 8th AIAA/CEAS Aeroacoustics Conference, Breckenridge, CO, 17-19 June, 2002.

Smirnov, A., Shi, S., Celik, I., Random Flow Generation Technique for Large Eddy Simulations and Particle-Dynamics Modelling, ASME J. of Fluids Engineering, 123:359-371, 2001.

Mani, R., The Influence of Jet Flow on Jet Noise, Journal of Fluid Mechanics, 74(5):753-793, 1976.

Balsa, T.F., The Acoustic Field of Sources in Shear Flow with Application to Jet Noise: Convective Amplification, Journal of Fluid Mechanics, 79(1):33-47, 1977.

Gliebe, P.R., T.F., Balsa, Aeroacoustics of Axisymmetric Single and Dual Flow Exhaust Nozzles, Journal of Aircraft, 15(11):743-749, 1978.

Curle, N., The Influence of Solid Boundaries upon Aerodynamic Sound. Proc. Roy. Soc., A, 231:505-514, 1970.

Larsson, J., Computational Aero Acoustics for Vehicle Applications, Licentiate, Chalmers University of Technology, Dept. of Thermo and Fluid Dynamics, 2002.

FfowcsWilliams, J.E., Hawkings, D.L., Sound generation by turbulence and surfaces in arbitrary motion, Philos. Trans. Roy. Soc. London Ser. A 264 (1969) 321–342.

Lighthill, M.J., On the Sound Generated Aerodynamically: I General Theory, Proc. Royal Soc. London, A. 211: 564-587, 1952.

Andersson, N., Eriksson, L., Davidson, L., Investigation of an Isothermal Mach 0.75 Jet and its Radiated Sound using Large-eddy Simulation and Kirchhoff Surface Integration, International Journal of Heat and Fluid Flow, 26, 393-410, 2005.

Engineering Science Data Unit (ESDU), Computer-based estimation procedure for single-stream jet noise: Including farfield, static jet mixing noise database for circular nozzles, ESDU: 98019, 2003.